Original Article
cnj.araku.ac.ir

☑ Cite This: Colloid Nanosci. J. 3(3) (2025) 652-668 DOI: 10.61882/CNJ.3.3.652

Dynamic viscosity and thermal conductivity modeling of nanofluids based on Eyring's absolute rate theory and modified Flory-Huggins equation

Alireza Fazlali*, Mohammad Mahdavi Nik

Department of Chemical Engineering, Arak University, Arak, Iran

ARTICLE INFO

Article History:
Received 2025-08-16
Revised 2025-10-22
Accepted 2025-11-01
Published 2025-11-06

Corresponding Authors:
Alireza Fazlali
Email:
a-fazlali@araku.ac.ir

ABSTRACT

Thermophysical properties such as dynamic viscosity and thermal conductivity play an important role in systems design calculations (equipment, processes, etc.) and in examining fluid properties. Over the past two decades, many experimental and semi-theoretical models have been proposed to calculate and predict thermophysical properties, especially viscosity and thermal conductivity of nanofluids, but none of these models has sufficient accuracy as a comprehensive model for calculating these properties. In this study a semi-theoretical relationship based on Eyring's absolute rate theory and the modified Flory-Huggins thermodynamics model based on the viscosity of the base fluid, molar volume of the base fluid and nanoparticle, temperature, volume fraction, and particle interaction parameter has been presented to model the dynamic viscosity of water-based nanofluids with Al_2O_3, CuO, SiO_2, TiO_2, Fe_3O_4, Ag, and Zr nanoparticles and ethylene glycol-based nanofluids with Al_2O_3, SiO_2, and ZnO nanoparticles. Using dimensional analysis, a new model based on the presented relationship for dynamic viscosity is presented to calculate the thermal conductivity of nanofluids based on the thermal conductivity of the base fluid and nanoparticles, molar volume of the base fluid and nanoparticles, temperature, specific heat capacity, volume fraction, and interaction parameter. The presented model is developed to calculate the thermal conductivity of water-based nanofluids with Al_2O_3, CuO, Fe_3O_4, TiO_2, and Ag nanoparticles, and also for ethylene glycol-based nanofluids with Al_2O_3, CuO, and ZnO nanoparticles. To develop the Eyring-mFH (Eyring-modified Flory-Huggins) model, experimental dynamic viscosity data of nanofluids with Newtonian behavior from different references in the temperature range of 10-90 °C and the volume fraction range of 0.2-9.4% were used to calculate the interaction parameters between the base fluid and nanoparticles in the viscosity model and experimental thermal conductivity data of different nanofluids in the temperature range of 10-90 °C and the volume fraction range of 0.3-8.6% were used to calculate the interaction parameter in the thermal conductivity model. The maximum and minimum errors of the model optimization on tentative data based on AARD% are 5.94% and 0.04% for the viscosity model, and 0.7% and 0.16% for the thermal conductivity model, respectively.

KEYWORDS: *Nanofluids; Viscosity; Thermal conductivity; Modeling; Eyring's absolute rate theory; Modified Flory-Huggins*

This work is licensed under the Creative Commons Attribution 4.0 International License.
To view a copy of this license, visit http://creativecommons.org/licenses/by/4.0/.

1. Introduction

Today, due to environmental challenges and technological development, common heat transfer fluids such as water, oil, air, and refrigerants such as Freon, etc., do not meet the need for heat transfer at high rates. In order to improve the thermal conductivity properties of liquids, solid particles in the size range of millimeters and micrometers were added to liquids, which significantly improved the thermal conductivity of fluids. However, these fluids had problems such as high pressure drop, sedimentation, and rapid clogging by solid particles. With the development of technology, the field of producing solid particles at the nanoscale was created [1]. In 1995, the concept of nanofluid was introduced by Choi et al. [2]. Nanofluid is a two-phase solid-liquid system in which solid nanoparticles on the scale of 1-100 nm are dispersed in a base fluid, which includes polymers, metals, metal oxides, etc. Base fluids are often the same as common heat transfer fluids, but other fluids, such as alcohols, have also been investigated [1]. Due to their smaller size and higher specific surface area, these particles have better distribution behavior, less clogging, and wear [3]. The application of nanofluids in thermal processes such as electronic cooling systems, fuel cells, temperature regulation of engines, solar collectors, chillers, and heat exchangers has been investigated [4]. In general, nanofluids can be studied and investigated from the perspectives of studying and modeling thermophysical properties, applications, and heat transfer modeling [3]. Modeling has always been of great importance in all sciences, especially in engineering sciences and techniques, to reduce costs, improve resource efficiency, decrease the duration of design processes, etc. Although numerous models have been proposed for predicting nanofluid viscosity and thermal conductivity, they often suffer from limited generality across different nanoparticle-base fluid combinations. A critical methodological gap exists in simultaneously accounting for both the hydrodynamic interactions (addressed by theories like Eyring's) and the thermodynamic non-idealities (addressed by models like Flory-Huggins) within a single, coherent framework. This gap limits their predictive accuracy and universal applicability. The principal novelty of this work is the first-time integration of Eyring's absolute rate theory with a modified Flory-Huggins model, establishing the Eyring-mFH framework. This is not merely a combination but a physicochemical unification that provides a more fundamental and generalized approach for modeling both dynamic viscosity and thermal conductivity of diverse nanofluids. The model development process consists of collecting a database of various nanofluids so that the data is in a wide range of temperature and volume fraction as much as possible. Then, programming is done in the form of minimizing the objective function in MATLAB software. Finally, the output report of the program is presented in the form of optimization error percent and demonstrating the results in the form of graphs and a comparison with other models.

2. Modeling

As mentioned, the purpose of presenting a new model for calculating the thermal conductivity and viscosity properties of nanofluids is to investigate the ability of this semi-theoretical model, considering the interaction parameter between nanoparticles and the base fluid in the form of a polymer thermodynamic model, in comparison with other models presented in recent years, as well as classical models. Since various parameters affect the thermophysical behavior of nanofluids, to increase the speed of calculations, reduce the required data, and the overall simplicity of the model, the following assumptions have been used for the model development process:

1- Nanofluid consists of a base fluid and a type of nanoparticle.

2- The nanoparticles are completely dispersed in the base fluid.

3- The excess molar volume due to mixing is considered zero.

These assumptions are also consistent with the assumptions of the modified Flory-Huggins thermodynamic model.

2.1. Development of the viscosity model

Based on Eyring's absolute reaction rates, which are presented for all rate processes, including chemical reaction kinetics, viscosity, diffusion, and electrochemical phenomena, when a system undergoes a chemical reaction or a rate process, the reactants initially form a pseudomolecule or activated complex in the initial state. When the initial system gains enough energy to cross the energy barrier, it collapses and reaches the final state. Eyring presented a relationship for the reaction rate, then defined viscosity based

on the absolute rate theory, in which the shear force acting on two layers of molecules causes flow when a molecule, by gaining activation free energy and crossing the energy barrier, displaces its neighboring molecule and is placed in a new equilibrium position that is like a hole. According to Eyring, there is a very close relationship between the excess activation free energy and the excess Gibbs free energy [5]. Finally, the Eyring viscosity model is given in Equation (1) [6].

$$\eta = \frac{hN}{V_m}\exp(\Delta g^{+}/RT) \tag{1}$$

In Equation (1), h, N, V_m, and Δg^{+} represent Planck's constant, Avogadro's number, molar volume, and Gibbs free energy of activation, respectively. The free energy of activation for motion in Equation (1) can be considered as the sum of an ideal part and an additional part:

$$\Delta g^{+} = \Delta g^{+,ideal} + g^{+,E} \tag{2}$$

According to Equation (1), the viscosity for an ideal system is equal to:

$$\eta_{m,ideal} = \frac{hN}{V_{m,ideal}}\exp(\frac{\Delta g^{+,ideal}}{RT}) \tag{3}$$

By rearranging Equation (3) and taking the logarithm of both sides, Equation (4) is obtained:

$$\frac{\Delta g^{+,ideal}}{RT} = \ln(\eta V)_{m,ideal} - \ln(hN) \tag{4}$$

Also, by combining Equations (2) and (1), an unrefined equation for viscosity of mixture is obtained:

$$\eta_m = \frac{hN}{V_m}\exp(\frac{\Delta g^{+,ideal}}{RT} + \frac{g^{+,E}}{RT}) \tag{5}$$

By rearranging Equation (5) and taking the logarithm of both sides, Equation (6) is obtained:

$$\ln(\eta V)_m = \ln(hN) + \frac{\Delta g^{+,ideal}}{RT} + \frac{g^{+,E}}{RT} \tag{6}$$

By combining Equations (4) and (6), the final dynamic viscosity relation for the non-ideal system is calculated:

$$\ln(\eta V)_m = \ln(\eta V)_{m,ideal} + \frac{g^{+,E}}{RT} \tag{7}$$

The first term on the right side of Equation (7) represents the ideal viscosity of the constituent components, while the second term accounts for the nonideality arising from interactions between them. The modified Flory-Huggins model is based on the lattice model, which is used to describe the phase behavior of systems with molecules of different sizes. Polymer systems consisting of solvent + polymer, in which the polymer macromolecules have a significant size difference from the solvent molecules, fall into this category. The excess molar Gibbs free energy of Flory-Huggins, obtained from the Gibbs energy relation, is given by (8) [7].

$$\frac{g^{E}}{RT} = x_1\ln(\frac{\varphi_1}{x_1}) + x_2\ln(\frac{\varphi_2}{x_2}) + \chi_{12}(x_1 + mx_2)\varphi_1\varphi_2 \tag{8}$$

$$m = \frac{V_{m,2}}{V_{m,1}} \tag{9}$$

In these relations, x, m and χ_{12} represent the mole fraction, the molar volume ratio of component 2 (polymer) to the molar volume of component 1 (solvent), and the interaction parameter between components 1 and 2, respectively, which is calculated using experimental data. The first and second terms on the right-hand side of Equation (8) represent the entropy of mixing, which calculates the effects of the geometry, size and shape of the molecules, and the third term represents the enthalpy of mixing, which takes into account the interactions between the molecules. By substituting Equation (8) into Equation (7) and rewriting in an applicable form for nanofluids including base fluid + nanoparticle, the final Eyring-mFH relation for the viscosity of nanofluids is obtained.

$$\ln(\eta V)_{nf} = \ln(\eta V)_{nf,ideal} + x_{bf}\ln(\frac{\varphi_{bf}}{x_{bf}}) + x_p\ln(\frac{\varphi_p}{x_p}) + \chi(x_{bf} + mx_p)\varphi_{bf}\varphi_p \tag{10}$$

The first term on the right side of Equation (10) is calculated using Equation (11) [8]:

$$\ln(\eta V)_{nf,ideal} = x_1 \ln(\eta V)_1 + x_2 \ln(\eta V)_2 \quad (11)$$

In this relation, viscosity is in mPa.s and molar volume is in cm^3/mol. Equation (12) is used to calculate V_{nf} in Equation (11):

$$V_{nf} = (1-\varphi_{bf})V_{bf} + \varphi_p V_p \quad (12)$$

Qian et al. [9] considered the interaction parameter χ as the product of two terms with temperature dependence D(T) and the polymer volume fraction (equivalent to the nanoparticle volume fraction) $B(\varphi_p)$, which is given in Equation (13).

$$\chi(T,\varphi_p) = (d_0 + d_1/T + d_2 \ln T).(1 + b_1\varphi_p + b_2\varphi_p^2) \quad (13)$$

In these relations, d_0, d_1, d_2, b_1 and b_2 are the constants of the binary system. A simpler relationship (12) was proposed by Bae et al. [10].

$$\chi(T,\varphi_p) = (d_0 + d_1/T + d_2 \ln T).(\frac{1}{1-b\varphi_p}) \quad (14)$$

The parameters to be optimized in the interaction term (χ) are empirical and no theoretical meaning has been found for them yet. In fitting and optimizing viscosity and thermal conductivity models, each of the aforementioned equations was used for the concentration dependence of the interaction parameter, and a comparison of the results is presented in the results and discussion section.

2.2 Development of the thermal conductivity model

Based on Equation (7), a relationship based on the analogy between the momentum diffusion coefficient and the thermal diffusion coefficient, and the dimensional correspondence of the parameter ηV in Equation (7) with the dimensions of a parameter in heat transfer concepts is presented:

$$\eta V \approx \frac{kM}{\rho C_p} \quad (15)$$

In this relation, M represents the molar mass. According to the analogy provided in Equation (15) and rewriting Equation (7), Equation (16) is obtained:

$$\ln(\frac{kM}{\rho C_p})_{nf} = \ln(\frac{kM}{\rho C_p})_{nf,ideal} + \frac{g^{+,E}}{RT} \quad (16)$$

The first term on the right side of Equation (16) represents the ideal thermal diffusivity, and the second term, which is calculated using the modified Flory-Huggins excess Gibbs energy equation, represents the non-ideal thermal diffusivity due to phenomena in nanofluids such as Brownian motion, nanoparticle aggregation, nanolayer effect, etc. The ideal thermal diffusivity is calculated as Equation (17):

$$\ln(\frac{kM}{\rho C_p})_{nf,ideal} = x_{bf} \ln(\frac{kM}{\rho C_p})_{bf} + x_p \ln(\frac{kM}{\rho C_p})_p \quad (17)$$

In this relation, χ is the binary interaction parameter of the base fluid molecule and the nanoparticle, which is calculated using experimental data. Density has the dimension g/cm^3, specific heat capacity has the dimension J/g.K, and thermal conductivity has the dimension W/m.K Equation (18) is used to calculate the expression $(\rho C_p/M)_{nf}$:

$$(\frac{\rho C_p}{M})_{nf} = \varphi_{bf}(\frac{\rho C_p}{M})_{bf} + \varphi_p(\frac{\rho C_p}{M})_p \quad (18)$$

It should be noted that at high concentrations of nanoparticles, there is a possibility of their aggregation, but the current models does not include a parameter to predict or determine the amount of aggregation.

3. Data collection and optimization

To perform the optimization process of the Eyring-mFH model to calculate the binary interaction parameter χ, an extensive database including viscosity and thermal conductivity data of nanofluids was collected. 579 experimental viscosity data and 152 experimental thermal conductivity data collected from various nanofluids were used in the optimization process. The values of density, thermal conductivity, specific heat capacity and molar mass of nanoparticles present in the nanofluids used in the optimization process are given in Table 1.

The experimental data used to develop the viscosity and thermal conductivity model, along with the nanoparticle size, nanoparticle volume

Table 1. Density, thermal conductivity, specific heat capacity, and molar mass values of nanoparticles [3, 11, 12].

Nanoparticle	ρ (g/cm^3)	k (W/m.K)	C_p (J/kg.K)	M
Al_2O_3	3.97	40	765	101.96
CuO	6.32	18	540	79.55
TiO_2	4.15	8.48	710	79.87
SiO_2	2.2	1.2	745	60.1
Ag	10.5	429	235	107.87
Zr	5.6	-	-	91.22
ZnO	5.61	50	504.7	81.38
Fe_3O_4	5.2	6	653.4	231.52

Table 2. Experimental viscosity data used in optimizing the Eyring-mFH viscosity model.

Nanofluid	Size (nm)	Volume fraction (%)	Temp (°C)
Water/Al_2O_3 [13]	47	1-9.4	21-70
Water/Al_2O_3 [13]	36	1-9.1	21-70
Water/CuO [13]	29	1-9	21-66
Water/TiO_2 [14]	21	0.2-3	13-55
Water/SiO_2 [15]	12	0.45-4	20-50
Water/Ag [11]	60	0.3-0.9	50-90
Water/Fe_3O_4 [16]	13	1-2	20-60
Water/Zr [12]	10	0.5-3	20-80
EG/Al_2O_3 [17]	43	0.5-6.6	10-50
EG/Al_2O_3 [17]	8	0.5-3.1	10-50
EG/ZnO [18]	48	0.5-4.7	10-50
EG/ZnO [18]	4.6	0.5-2.1	10-50
EG/SiO_2 [19]	25	0.5-3	30-50

Table 3. Experimental thermal conductivity data used in the optimization of the Eyring-mFH thermal conductivity model.

Nanofluid	Size (nm)	Volume fraction (%)	Temp (°C)
Water/Al_2O_3 [20]	25	1-5	15-55
Water/CuO [21]	31	0.5-1	20-50
Water/Fe_3O_4 [16]	13	0.4-2	20-60
Water/TiO_2 [22]	21	0.6-2	15-35
Water/Ag [11]	60	0.3-0.9	50-90
EG/Al_2O_3 [17]	43	3.1-8.6	10-50
EG/CuO [21]	31	0.5-1	20-50
EG/ZnO [18]	48	1-4.7	10-70

fraction in the nanofluid, and system temperature, are presented in Tables 2 and 3, respectively.

The objective function defined in the optimization process is given in Equation (19):

$$OF = \sum_{i=1}^{NP} \left(y_i^{calc} - y_i^{\exp} \right)^2 \tag{19}$$

To evaluate the accuracy of the models, the average absolute relative deviation (AARD%), root mean square error (RMSE), and maximum deviation (MD) are used. The formula for this errors are presented in Equations (20-22):

$$AARD\% = \frac{1}{n} \sum_{i=1}^{NP} \frac{\left| y_i^{\exp} - y_i^{calc} \right|}{y_i^{\exp}} \times 100 \tag{20}$$

$$RMSE = \sqrt{\frac{\sum_{i=1}^{NP} (y_i^{\exp} - y_i^{calc})^2}{n}} \tag{21}$$

$$MD = \max\left(\left| y_i^{\exp} - y_i^{calc} \right| \right) \tag{22}$$

4. Results and Discussion

The results of the optimization of the Eyring-mFH model for the viscosity and thermal conductivity of nanofluids are presented in three ways. First, the results of the optimized parameters along with AARD%, RMSE, and maximum deviation are presented for all the nanofluids studied using both the interaction relations (13) and (14). After choosing the best relation to express the concentration dependence of the interaction parameter, the performance of the Eyring-mFH model is displayed graphically in comparison with the experimental data. Then, for each nanofluid, a comparison is made between the presented model and the models that have been expressed so far by other researchers. The results of the optimization of the Eyring-mFH model on the viscosity experimental data mentioned in Table 2 are given in Tables 4 and 5. The results are also presented graphically in Fig. 1 and Fig. 2.

The results of the optimization of the Eyring-mFH model on the experimental thermal conductivity data mentioned in Table 3 are given in Tables 6 and 7. The results are also presented graphically in Fig. 3 and Fig. 4.

For further evaluation, the Eyring-mFH viscosity

Table 4. Interaction constants, AARD%, RMSE, and maximum deviation of the Eyring-mFH model for calculating viscosity with the interaction parameter $\chi = (\frac{1}{1-b_1\varphi_p})(d_0 + d_1/T + d_2 \ln T)$.

Nanofluid	Size	b_1	d_0	d_1	d_2	AARD%	RMSE	MD
Water/Al_2O_3	47 nm	6.748	-1251.55	60203.62	185.547	5.33	0.0841	0.2577
Water/Al_2O_3	36 nm	6.256	-1856.55	88547.99	275.184	2.06	0.0355	0.1082
Water/CuO	29 nm	5.51	-3562.33	171163.7	527.454	4.2	0.0707	0.1798
Water/TiO_2	21 nm	13.122	-1417.09	69220.51	211.254	1.33	0.0178	0.0381
Water/SiO_2	12 nm	6.429	1612.955	-76088.3	-232.849	2.4	0.031	0.0662
Water/Ag	60 nm	-55.072	19909	-1079548	-2860.75	0.72	0.0052	0.0184
Water/Fe_3O_4	13 nm	-57.687	-10559.9	457150.4	1594.675	1.99	0.0273	0.0633
Water/Zr	10 nm	-7.676	-23.537	5370.44	9.566	0.14	0.0016	0.0038
EG/Al_2O_3	43 nm	0.347	-3619.62	172427.5	538.88	1.77	0.5365	1.0606
EG/Al_2O_3	8 nm	-3.702	-6623.67	321008.3	981.21	1.6	0.4918	1.2166
EG/ZnO	48 nm	-0.918	-6448.32	305040.6	958.889	1.67	0.4294	1.5448
EG/ZnO	4.6 nm	-4.091	163.2	-7.145	-20.137	1.66	0.436	0.942
EG/SiO_2	25 nm	11.04	14746.37	-660800	-2195.062	2.73	0.4687	1.2148
					Average	2.12	0.2027	0.5165

Table 5. Interaction constants, AARD%, RMSE, and maximum deviation of the Eyring-mFH model for calculating viscosity with the interaction parameter $\chi = (1 + b_1\varphi_p + b_2\varphi_p^{\,2})(d_0 + d_1/T + d_2 \ln T)$.

Nanofluid	Size	b_1	b_2	d_0	d_1	d_2	AARD%	RMSE	MD
Water/Al_2O_3	47 nm	-18.529	188.03	-3700.62	178141.7	548.576	5.94	0.0679	0.1642
Water/Al_2O_3	36 nm	-8.334	161.89	-2724.13	129926.3	403.78	2.13	0.0343	0.1078
Water/CuO	29 nm	33.433	2.458	-1779.56	85414.29	263.434	1.82	0.0476	0.1735
Water/TiO_2	21 nm	12.855	335.859	-1382.46	67538.66	206.091	1.33	0.0177	0.0379
Water/SiO_2	12 nm	118.54	-1663.66	698.70	-32937.4	-100.86	1.07	0.017	0.0338
Water/Ag	60 nm	-25.755	-526.184	18299.08	-992198	-2629.45	0.67	0.005	0.0174
Water/Fe_3O_4	13 nm	-54.137	1267.024	-11519.9	498435.4	1739.96	1.91	0.0253	0.0554
Water/Zr	10 nm	-8.678	70.102	-23.843	5439.553	9.689	0.04	0.0004	0.001
EG/Al_2O_3	43 nm	-4.277	48.741	-3988.52	190017.6	593.804	1.12	0.3501	1.0476
EG/Al_2O_3	8 nm	-5.725	58.043	-6770.49	328114.9	1002.962	1.6	0.4887	1.1275
EG/ZnO	48 nm	-6.125	82.356	-6955.09	329033	1034.24	1.56	0.3506	1.2482
EG/ZnO	4.6 nm	-19.379	525.965	178.940	188.983	-21.985	1.61	0.3974	0.747
EG/SiO_2	25 nm	80.15	-1014.53	8907.447	-399247	-1325.89	2.52	0.415	0.9944
						Average	1.91	0.1705	0.4427

Table 6. Interaction constants,.AARD%, RMSE, and maximum deviation of the Eyring-mFH model for calculating thermal conductivity with the interaction parameter $\chi = (\frac{1}{1-b_1\varphi_p})(d_0 + d_1/T + d_2 \ln T)$.

Nanofluid	Size	b_1	d_0	d_1	d_2	AARD%	RMSE	MD
Water/Al_2O_3	25 nm	-5.11×10^{20}	-1.14×10^{22}	3.75×10^{23}	1.78×10^{21}	0.79	0.0064	0.0125
Water/CuO	31 nm	-125.903	2727.99	-155856	-386.802	0.29	0.0027	0.0054
Water/Fe_3O_4	13 nm	-194.383	1099.08	-593534	-1570.6	0.75	0.0074	0.0147
Water/TiO_2	21 nm	-27.292	165.255	-178.625	-29.105	0.24	0.0018	0.0042
Water/Ag	60 nm	-59.564	17011.96	-1095054	-2353.66	0.59	0.0072	0.0204
EG/Al_2O_3	43 nm	0.69	4.01	17.384	-2.369	0.55	0.0017	0.003
EG/CuO	31 nm	60.334	692.401	-37904.4	-99.688	0.57	0.0019	0.0039
EG/ZnO	48 nm	-1.402	-1181.76	50257.52	174.902	0.71	0.0024	0.0044
					Average	0.56	0.004	0.0086

Table 7. Interaction constants, AARD%, RMSE, and MD of the Eyring-mFH model for calculating thermal conductivity with the interaction parameter $\chi = (1 + b_1\varphi_p + b_2\varphi_p^{\,2})(d_0 + d_1/T + d_2 \ln T)$.

Nanofluid	Size	b_1	b_2	d_0	d_1	d_2	AARD%	RMSE	MD
Water/Al_2O_3	25 nm	-38.612	431.893	-3088.25	100409.7	483.05	0.79	0.0059	0.0128
Water/CuO	31 nm	-298.98	19920.29	137741.1	-1.2×10^{7}	-16795.3	0.29	0.0027	0.0054
Water/Fe_3O_4	13 nm	-60.775	1284.046	7462.761	-402369	-1065.87	0.5	0.0049	0.0105
Water/TiO_2	21 nm	-24.303	356.254	164.261	-200.775	-28.915	0.24	0.0018	0.0042
Water/Ag	60 nm	-80.158	3884.95	18796.52	-1209016	-2601.07	0.47	0.0051	0.0112
EG/Al_2O_3	43 nm	-3.793	34.799	122.1	-5269.87	-20.222	0.55	0.0005	0.0009
EG/CuO	31 nm	297.287	7225.761	371.76	-20351.3	-53.523	0.57	0.0019	0.0039
EG/ZnO	48 nm	-6.594	80.304	-1284.52	54629.03	190.113	0.71	0.0021	0.0046
						Average	0.44	0.003	0.007

model has been compared with experimental data and models presented by other researchers, namely the models of Akande et al. [23], Klazly and Bognar [24], Garoosi [3], Hosseini et al. [25], and Batchelor [26]. The thermal conductivity model has been compared with the models of Hamilton and Crosser [27], Prasher et al. [28], Moghaddasi et al. [29], Hosseini et al. [30], and Garoosi [3]. The aforementioned models have been selected in such a way that the current model can be compared with theoretical, semi-theoretical, and empirical models presented over the past decades, each of which has considered various parameters in their models. The results of the comparisons for the viscosity model are presented in Fig. 5 and Fig. 6, and for the thermal conductivity model in Fig. 7 and Fig. 8.

By performing the optimization process and calculating and comparing the error values presented in Table 4 to Table 7, It is clear that the five-parameter relationship of the interaction parameter χ, Equation (13), has more favorable results than the four-parameter relationship, Equation (14), for viscosity and thermal conductivity models. The four-parameter viscosity model has average errors of 2.12%, 0.2027, and 0.5165 While the five-parameter viscosity model has average errors of 1.91%, 0.1705, and 0.4427 based on AARD%, RMSE, and MD, respectively. The four-parameter thermal conductivity model has average errors of 0.56%, 0.004, and 0.0086 While the five-parameter viscosity model has average errors of 0.44%, 0.003, and 0.007 based on AARD%, RMSE, and MD, respectively. Due to the large number of systems and the diversity in the volume fractions studied, four of the systems were investigated at low concentrations in Figs. 5.a, 6.f, 7.a, and 8.d. The models are only applicable within the studied temperature and volume fraction ranges (eg., Table 2 and Table 3), extrapolation beyond these ranges is not recommended.

A critical analysis of the comparative models performance reveals that their predictive accuracy is intrinsically linked to their underlying physical assumptions, which may align with or oversimplify the complex reality of nanofluids depending on

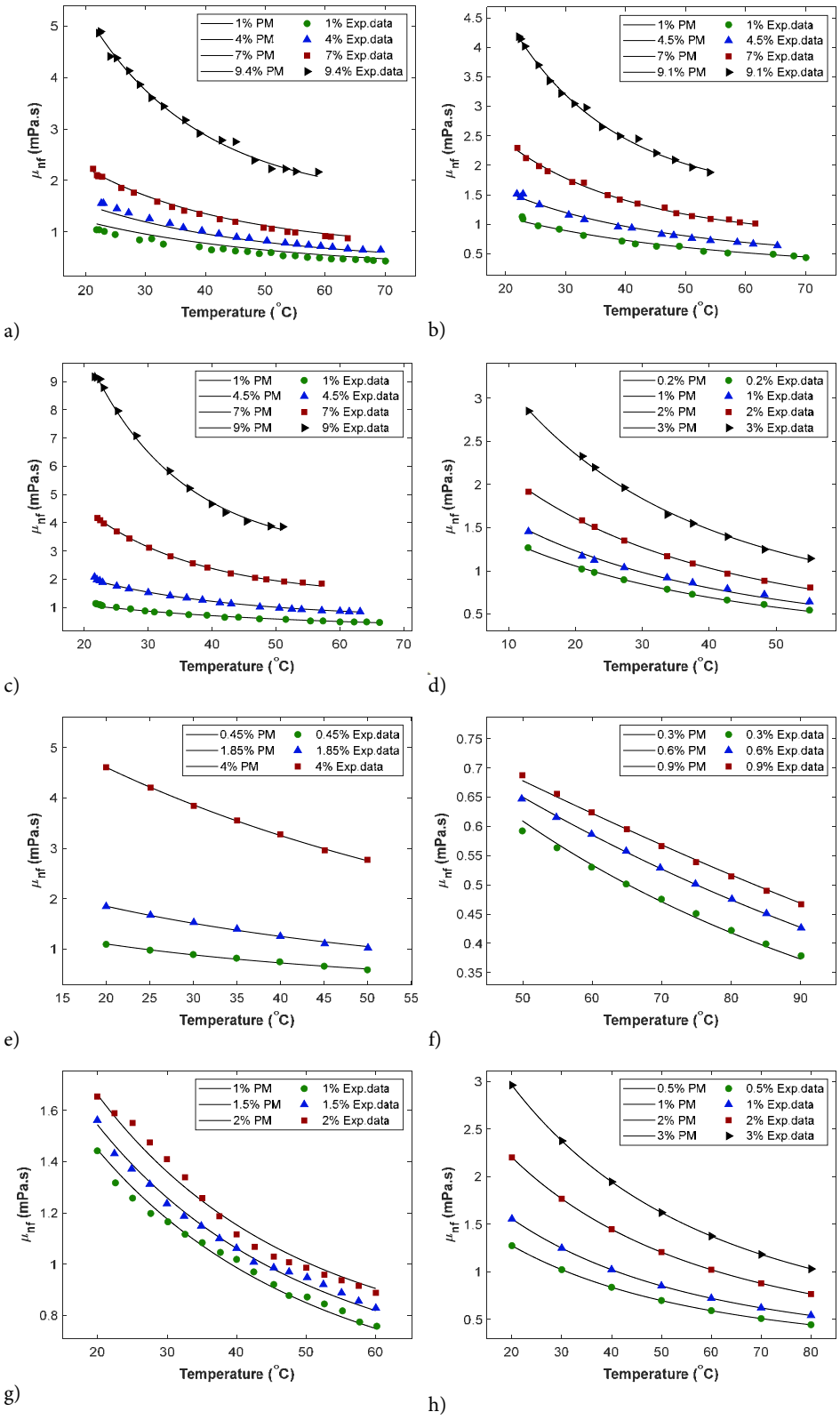

Fig. 1. Dynamic viscosity of water-base nanofluids. a) Water/Al_2O_3 (47 nm), b) Water/Al_2O_3 (36 nm), c) Water/CuO (29 nm), d) Water/TiO_2 (21 nm), e) Water/SiO_2 (12 nm), f) Water/Ag (60 nm), g) Water/Fe_3O_4 (13 nm), h) Water/Zr (10 nm).

the system and conditions. The classical Batchelor model [26], which considers only the hydrodynamic effect of non-interacting spherical particles, performs reasonably well at low volume fractions where aggregation is minimal. However, its failure at higher concentrations underscores its inability to capture dominant phenomena such as particle aggregation and the resulting complex hydrodynamic interactions, which significantly enhance viscosity. The Hamilton-Crosser model [27], a static model based solely on volume fraction and component conductivities, consistently

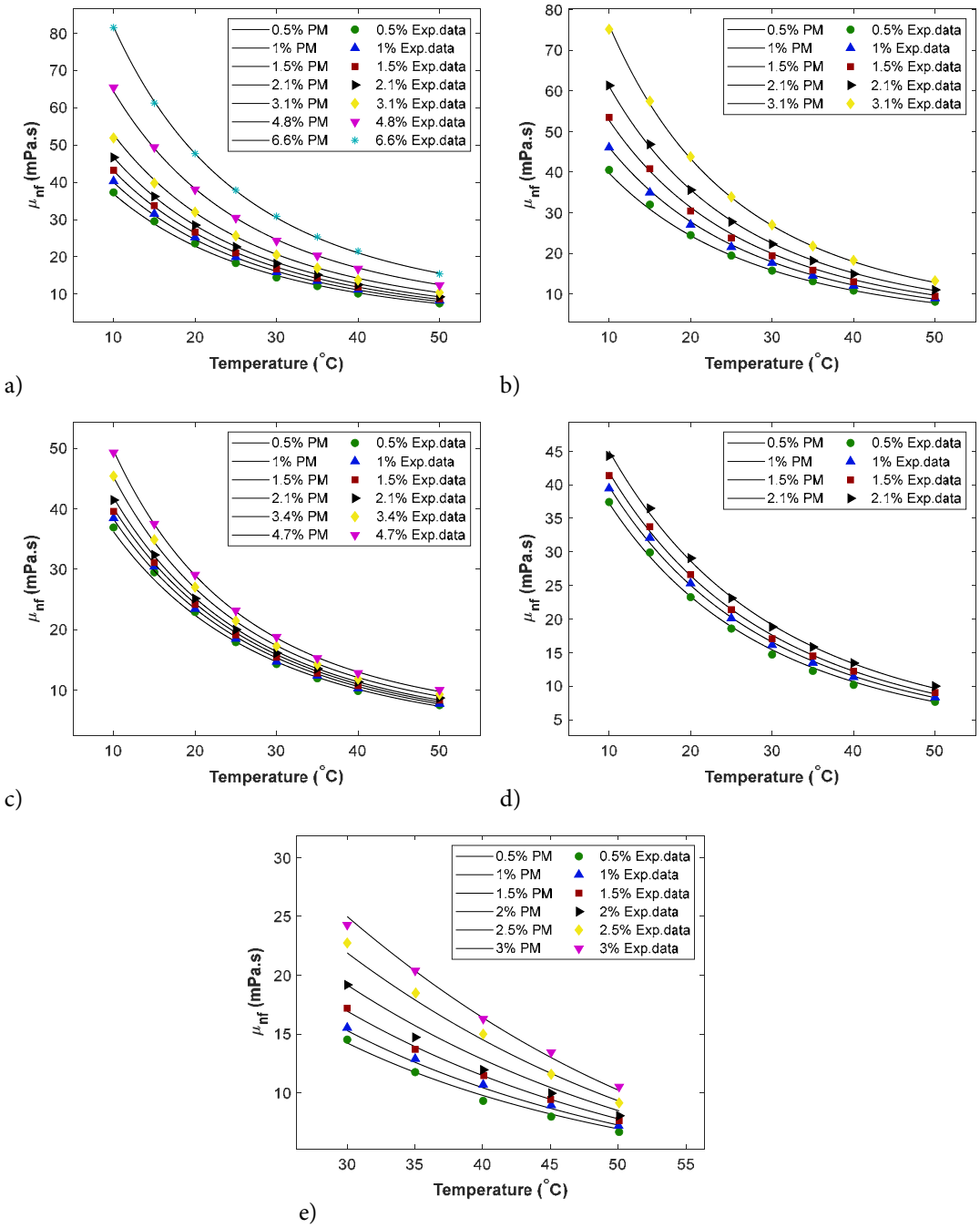

Fig. 2. Dynamic viscosity of EG-base nanofluids. a) EG/Al_2O_3 (43 nm), b) EG/Al_2O_3 (8 nm), c) EG/ZnO (48 nm), d) EG/ZnO (4.6 nm), e) EG/SiO_2 (25 nm).

underpredicts thermal conductivity as it inherently neglects dynamic enhancement mechanisms. The absence of contributions from Brownian motion-induced microconvection and the interfacial nanolayer renders it inadequate for capturing the true thermal behavior of nanofluids. Semi-empirical models like that of Prasher et al. [28], which attempt to incorporate Brownian motion, represent a step forward. Their variable performance, however, suggests that their simplified treatment of this complex phenomenon or their neglect of specific nanoparticle-base fluid

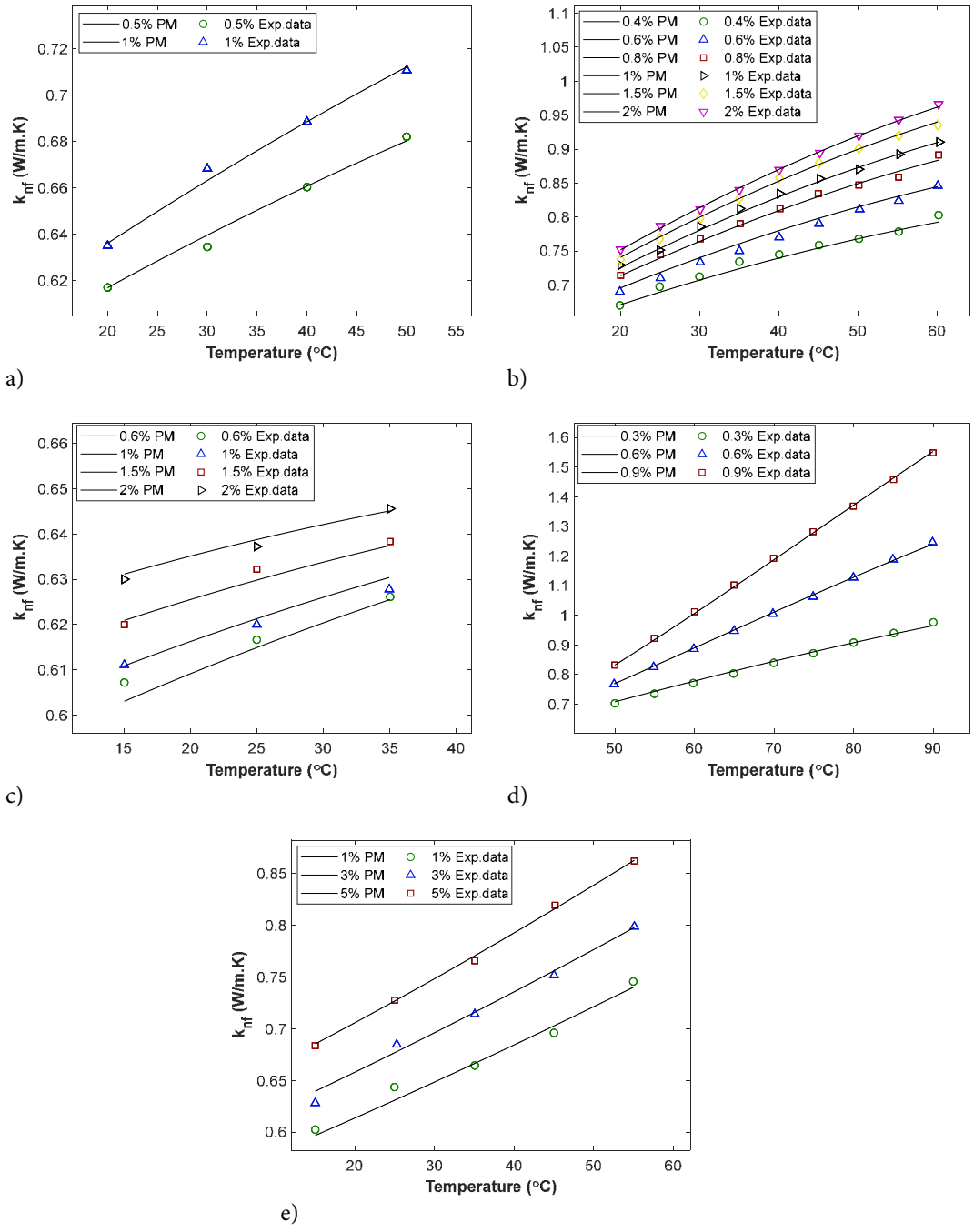

Fig. 3. Thermal conductivity of water-base nanofluids. a) Water/CuO (31 nm), b) Water/Fe_3O_4 (13 nm), c) Water/TiO_2 (21 nm), d) Water/Ag (60 nm), e) Water/Al_2O_3 (25 nm).

thermodynamic interactions (as captured by the Eyring-mFH model) limits their generality. The relatively strong performance of the Hosseini et al. model [30], which utilizes a thermodynamic model (NRTL), highlights the critical role of molecular-level interactions, a concept central to our Eyring-mFH approach. The superior accuracy of our model likely stems from its more fundamental physicochemical integration of viscous flow kinetics (Eyring) and thermodynamic non-ideality (mFH) within a unified framework, further validated by its successful extension to thermal conductivity via a novel dimensional analogy.

While the Eyring-mFH model demonstrates superior accuracy, this comes at the cost of a higher computational burden compared to purely empirical correlations. A quantitative analysis revealed that a single viscosity or thermal conductivity calculation for a specific nanofluid composition and temperature using the full Eyring-mFH framework requires approximately 0.5 to 1 second on a standard LapTop (using MATLAB R2022b on a system with an Intel Core i5 (12th Gen) processor and 16 GB RAM).

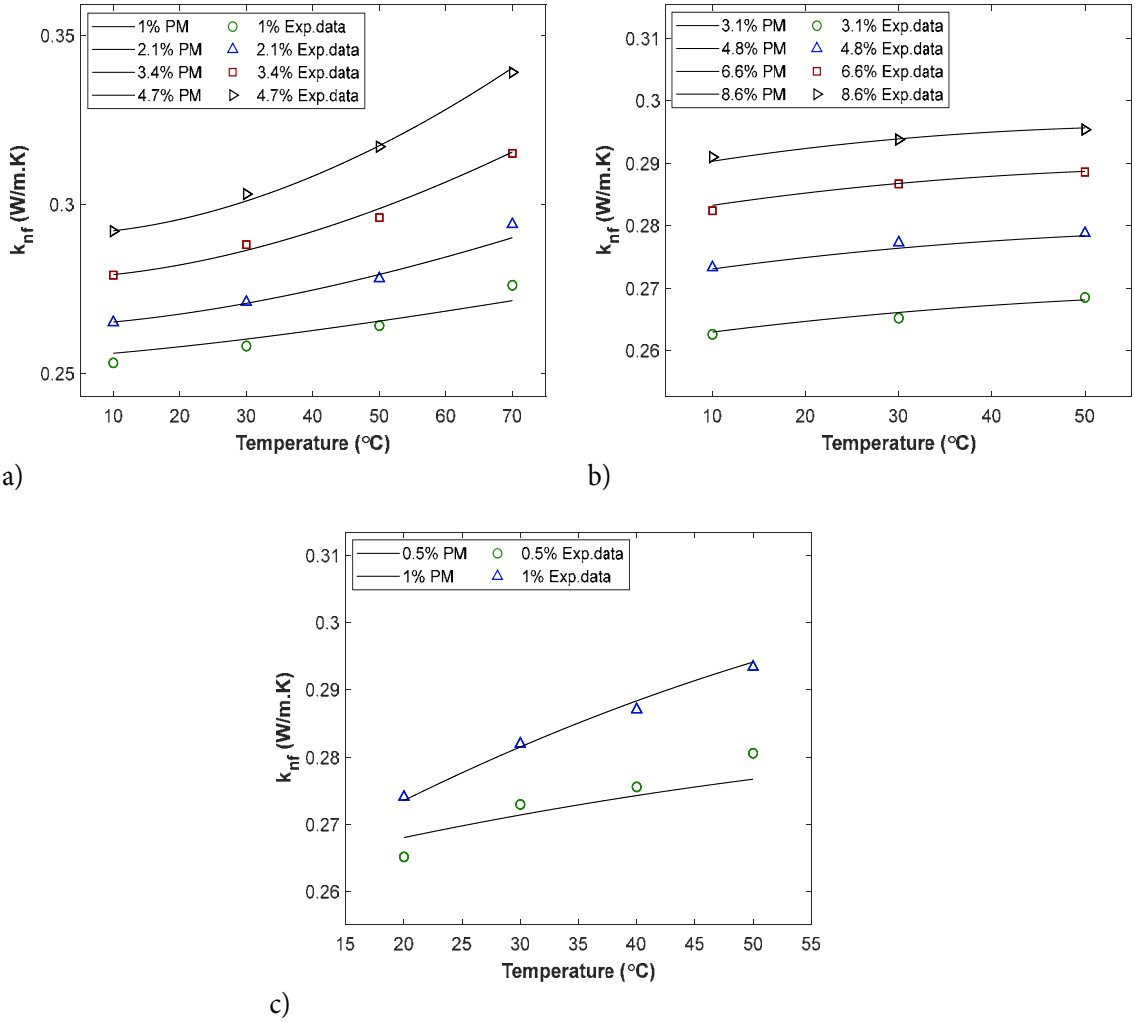

Fig. 4. Thermal conductivity of EG-base nanofluids. a) EG/ZnO (48 nm), b) EG/Al_2O_3 (43 nm), c) EG/CuO (31 nm).

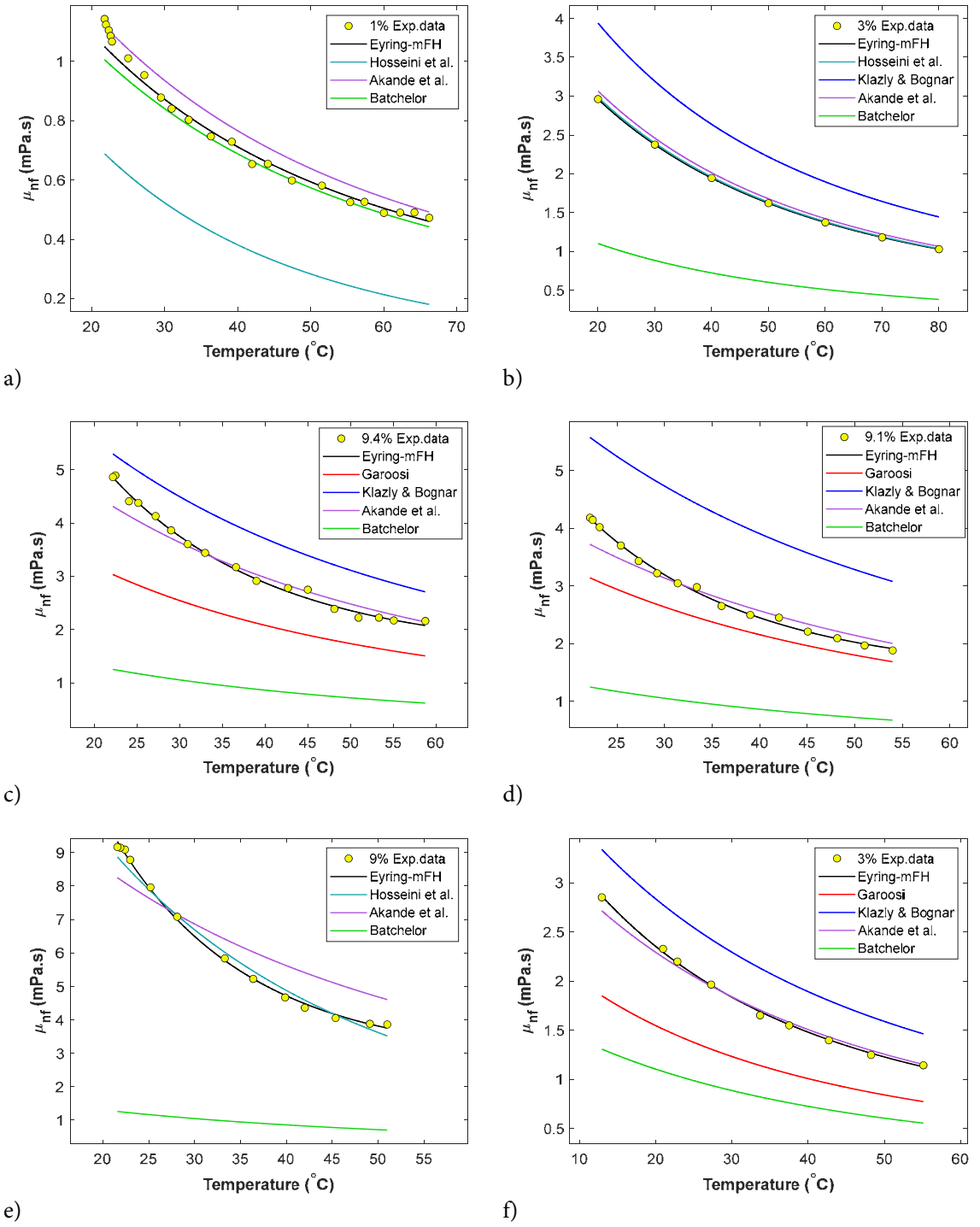

Fig. 5. Comparison of the Eyring-mFH viscosity model with another presented models for water-base nanofluids. a,e) Water-CuO (29 nm), b) Water-Zr (10 nm), c) Water-Al_2O_3 (47 nm), d) Water-Al_2O_3 (36 nm), f) Water-TiO_2 (21 nm), g) Water-SiO_2 (36 nm), h) Water-Ag (60 nm), i) Water-Fe_3O_4 (13 nm).

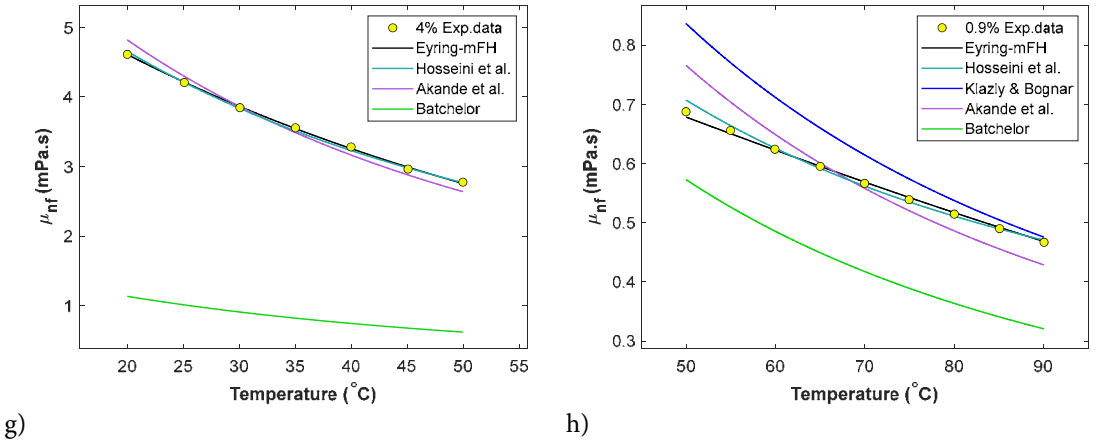

g) h)

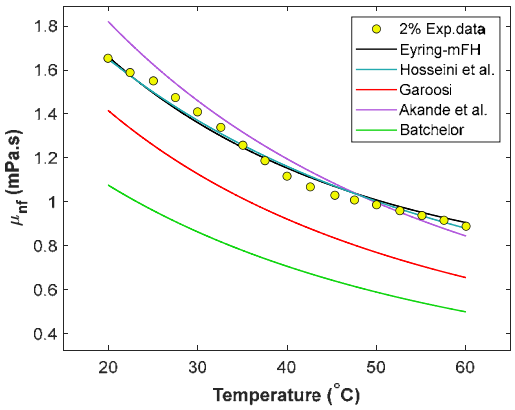

i)

Continued Fig. 5. Comparison of the Eyring-mFH viscosity model with another presented models for water-base nanofluids. a,e) Water-CuO (29 nm), b) Water-Zr (10 nm), c) Water-Al_2O_3 (47 nm), d) Water-Al_2O_3 (36 nm), f) Water-TiO_2 (21 nm), g) Water-SiO_2 (36 nm), h) Water-Ag (60 nm), i) Water-Fe_3O_4 (13 nm).

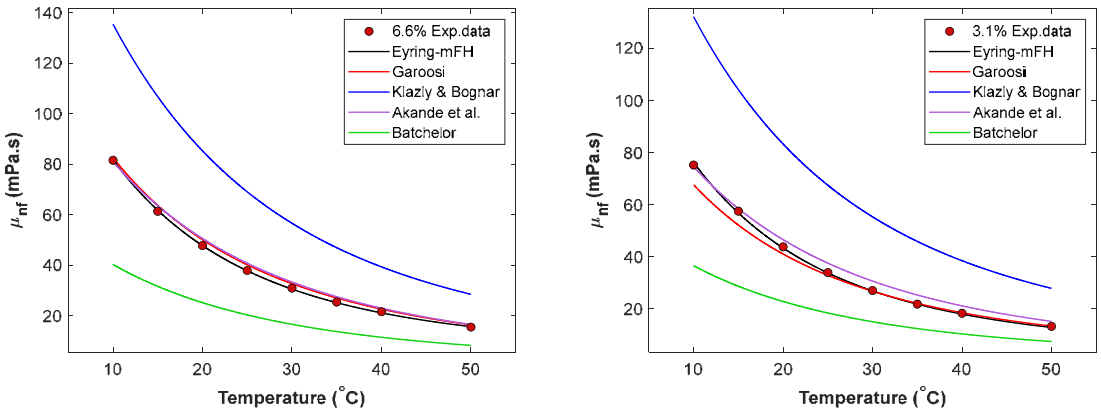

a) b)

Fig. 6. Comparison of the Eyring-mFH viscosity model with another presented models for EG-base nanofluids. a) Eg-Al_2O_3 (43 nm), b) Eg-Al_2O_3 (8 nm), c,f) Eg-ZnO (48 nm), d) Eg-ZnO (4.6 nm), e) Eg-SiO_2 (25 nm).

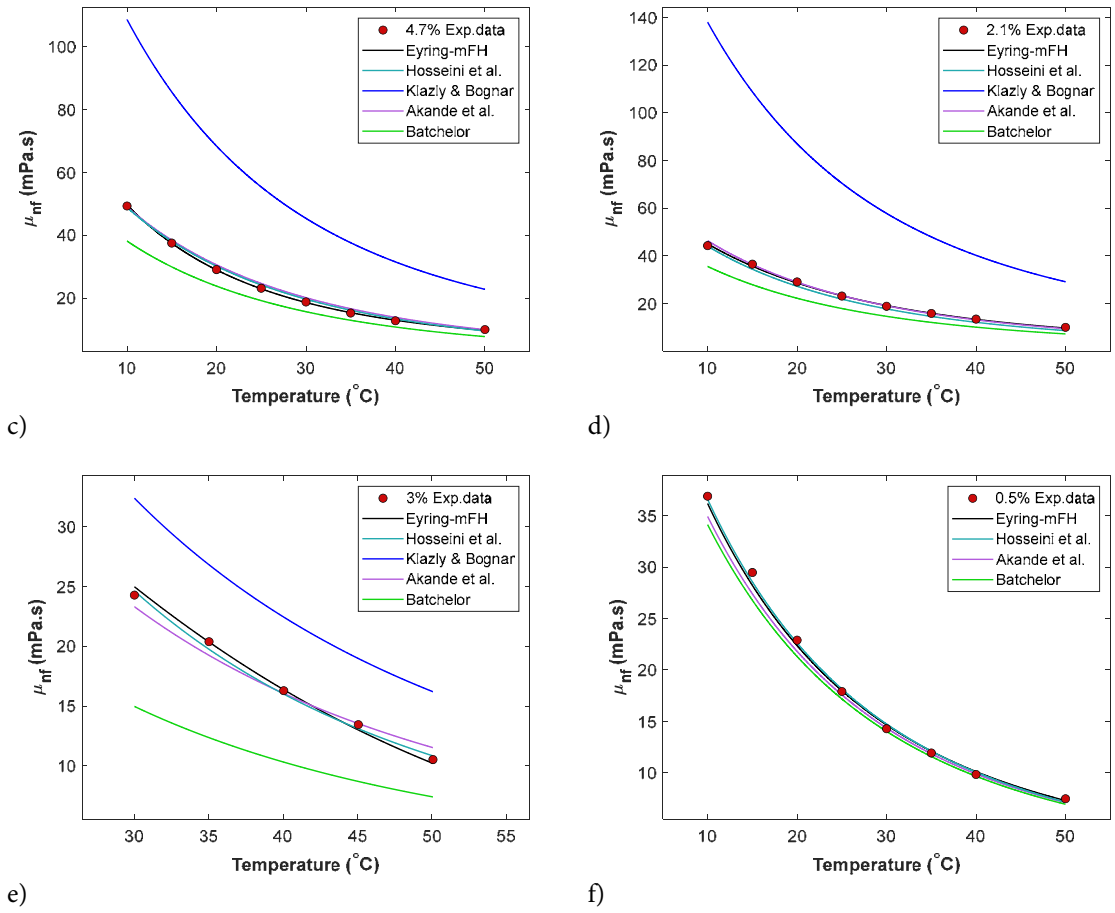

Continued Fig. 6. Comparison of the Eyring-mFH viscosity model with another presented models for EG-base nanofluids. a) Eg-Al_2O_3 (43 nm), b) Eg-Al_2O_3 (8 nm), c,f) Eg-ZnO (48 nm), d) Eg-ZnO (4.6 nm), e) Eg-SiO_2 (25 nm).

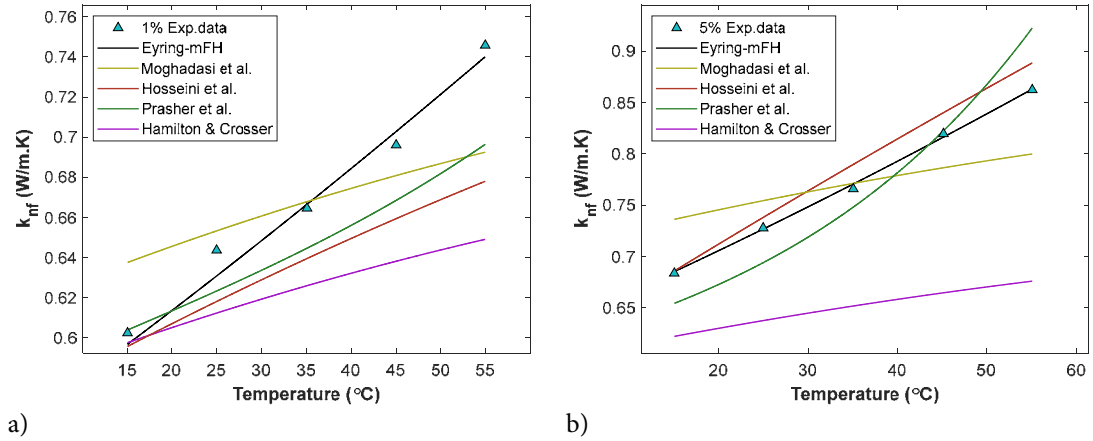

Fig. 7. Comparison of the Eyring-mFH thermal conductivity model with another presented models for water-base nanofluids. a,b) Water-Al_2O_3 (25 nm), c) Water-CuO (31 nm), d) Water-Fe_3O_4 (13 nm), e) Water-TiO_2 (21 nm), f) Water-Ag (60 nm).

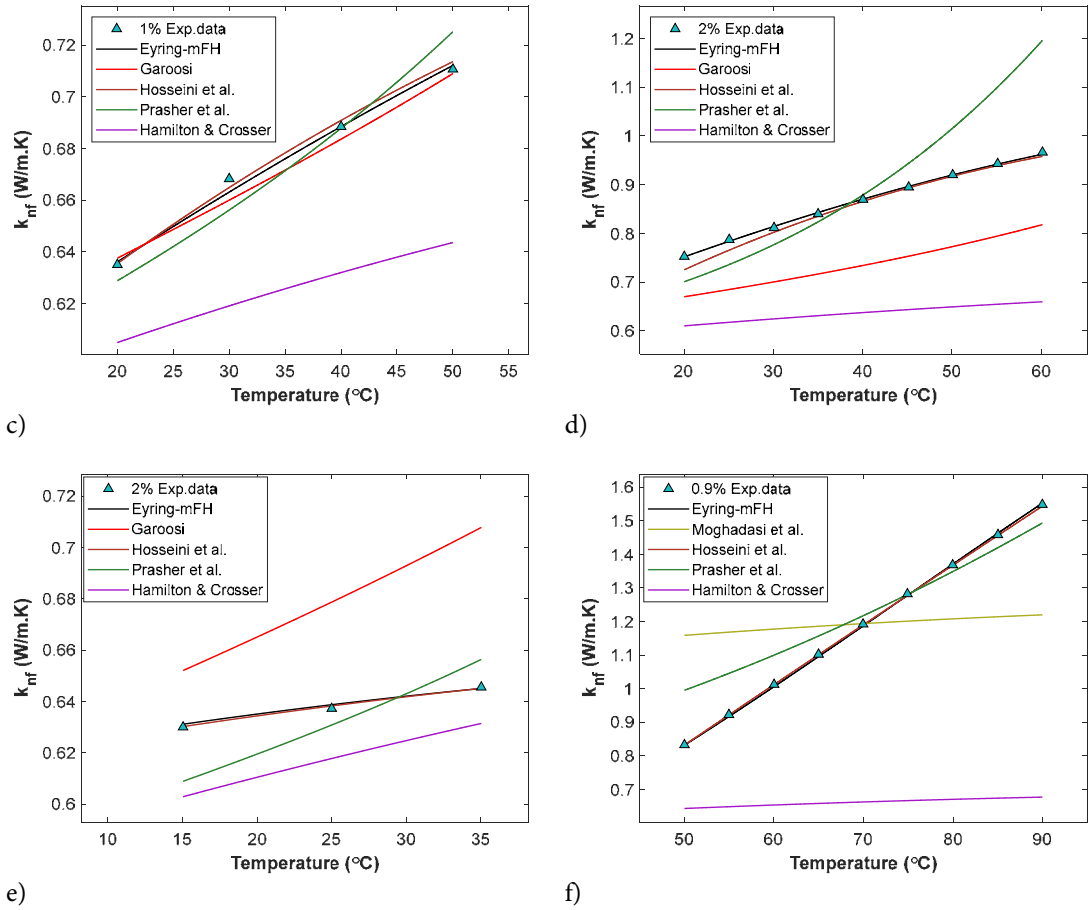

Fig. 7. Comparison of the Eyring-mFH thermal conductivity model with another presented models for water-base nanofluids. a,b) Water-Al_2O_3 (25 nm), c) Water-CuO (31 nm), d) Water-Fe_3O_4 (13 nm), e) Water-TiO_2 (21 nm), f) Water-Ag (60 nm).

5. Conclusion

This study successfully established the Eyring-mFH framework, a semi-theoretical model that unifies Eyring's absolute rate theory with a modified Flory-Huggins thermodynamic model for predicting the dynamic viscosity and thermal conductivity of nanofluids. The key achievement is the physically coherent integration of hydrodynamic and thermodynamic interactions into a single model, which grants it superior generality and accuracy across a wide range of nanoparticle-base fluid combinations compared to existing models.

Despite its strong performance, the models applicability is bounded by its underlying assumptions. The assumptions of perfect nanoparticle dispersion (no aggregation) and zero excess molar volume are its primary limitations, which may lead to deviations in real-world systems prone to aggregation, especially at high volume fractions. Furthermore, the current model was developed and validated for Newtonian nanofluids and may not capture the shear-thinning or thickening behavior of more complex non-Newtonian suspensions.

The following can be mentioned to clarify the future direction of this research:

-Extension to Non-Newtonian Nanofluids: The core framework can be adapted to incorporate shear-rate dependence, potentially by making the interaction parameter (χ) a function of shear rate.

-Application to Hybrid Nanofluids: The model can be tested and extended for nanofluids containing hybrid nanoparticles (e.g., SiO_2-TiO_2), which would require a more complex formulation to account for interactions between different nanoparticle types.

-Development of Machine-Learning (ML)

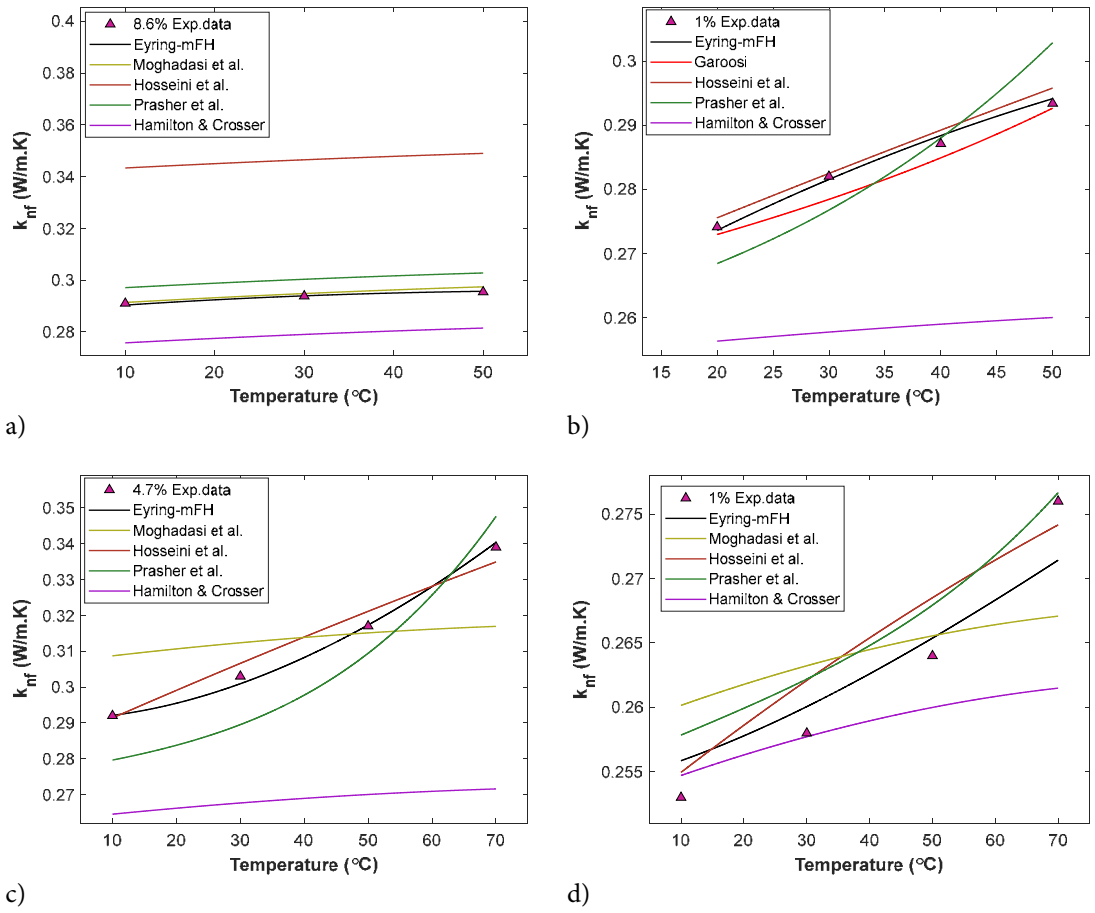

Fig. 8. Comparison of the Eyring-mFH thermal conductivity model with another presented models for EG-base nanofluids. a) EG-Al_2O_3 (43 nm), b) EG-CuO (31 nm), c,d) EG-ZnO (48 nm).

Hybrid Models: The physical grounding of the Eyring-mFH model makes it an ideal base for powerful hybrid modeling. Future work will explore using ML algorithms (e.g., neural networks) to accurately predict the temperature and concentration-dependent interaction parameters (b_1, b_2 d_0, d_1, d_2) from nanoparticle and base fluid properties. This would transform the model into a purely predictive tool, eliminating the need for parameter fitting from experimental data for new nanofluid systems.

Conflicts of Interest

The authors declare that there is no conflict of interests.

Nomenclature

Volume fraction	φ
Molar fraction	x
Mass fraction	w
Thermal conductivity	k (W/m.K)
Viscosity	η (mPa.s)
Density	ρ (kg/m^3, g/cm^3, mol/cm^3)
Interaction parameter	χ
Constants	b,d
Heat capacity	C_p (J/g.K)
Gas global constant	R (J/mol.K)
Molar volume	V (cm^3/mol)
Molar mass	M (g/mol)
Gibbs free energy	$g,\Delta g$ (J/mol)
Planck's constant	h
Avogadro's number	N
Subscripts	
Nanofluid	nf

Nanoparticle	*p*
Basefluid	*bf*
Counter	*i*
Mixture	*m*
Superscripts	
Activation	+
Excess	*E*
Number of points	*NP*

References

[1] J. Li, X. Zhang, B. Xu, M. Yuan, Nanofluid research and applications: A review, Int. Commun. Heat Mass Transf. 127 (2021) 105543. https://doi.org/10.1016/j.icheatmasstransfer.2021.105543

[2] S.U. Choi, Enhancing thermal conductivity of fluids with nanoparticles, Proc. ASME Int. Mech. Eng. Congr. Expo. 17421 (1995) 99–105. https://doi.org/10.1115/IMECE1995-0926

[3] F. Garoosi, Presenting two new empirical models for calculating the effective dynamic viscosity and thermal conductivity of nanofluids, Powder Technol. 366 (2020) 788–820. https://doi.org/10.1016/j.powtec.2020.03.032

[4] S. Hassani, R. Saidur, S. Mekhilef, A. Hepbasli, A new correlation for predicting the thermal conductivity of nanofluids using dimensional analysis, Int. J. Heat Mass Transf. 90 (2015) 121–130. https://doi.org/10.1016/j.ijheatmasstransfer.2015.06.040

[5] R. Powell, W. Roseveare, H. Eyring, Diffusion, thermal conductivity, and viscous flow of liquids, Ind. Eng. Chem. 33 (1941) 430–435. https://doi.org/10.1021/ie50376a003

[6] R.J. Martins, M.J.D.M. Cardoso, O.E. Barcia, Excess Gibbs free energy model for calculating the viscosity of binary liquid mixtures, Ind. Eng. Chem. Res. 39 (2000) 849–854. https://doi.org/10.1021/ie990398b

[7] J.M. Prausnitz, R.N. Lichtenthaler, E.G. Azevedo, Molecular Thermodynamics of Fluid-Phase Equilibria, 3rd ed., Prentice Hall PTR, 1998.

[8] Y.G. Wang, D.X. Chen, X.K. OuYang, Viscosity calculations for ionic liquid–cosolvent mixtures based on Eyring's absolute rate theory, J. Chem. Eng. Data 55 (2010) 4878–4884. https://doi.org/10.1021/je100487m

[9] C. Qian, S.J. Mumby, B. Eichinger, Phase diagrams of binary polymer solutions and blends, Macromolecules 24 (1991) 1655–1661. https://doi.org/10.1021/ma00007a031

[10] Y. Bae, J. Shim, D. Soane, J.M. Prausnitz, Representation of vapor–liquid and liquid–liquid equilibria for polymer systems, J. Appl. Polym. Sci. 47 (1993) 1193–1206. https://doi.org/10.1002/app.1993.070470707

[11] L. Godson, B. Raja, D.M. Lal, S. Wongwises, Experimental investigation on thermal conductivity and viscosity of silver nanofluid, Exp. Heat Transf. 23 (2010) 317–332. https://doi.org/10.1080/08916150903564796

[12] U. Rea, T. McKrell, L.W. Hu, J. Buongiorno, Laminar convective heat transfer of nanofluids, Int. J. Heat Mass Transf. 52 (2009) 2042–2048. https://doi.org/10.1016/j.ijheatmasstransfer.2008.10.025

[13] C. Nguyen et al., Temperature and particle-size dependent viscosity data, Int. J. Heat Fluid Flow 28 (2007) 1492–1506. https://doi.org/10.1016/j.ijheatfluidflow.2007.02.004

[14] A. Turgut et al., Thermal conductivity and viscosity of TiO_2 nanofluids, Int. J. Thermophys. 30 (2009) 1213–1226. https://doi.org/10.1007/s10765-009-0594-2

[15] I. Tavman et al., Viscosity and thermal conductivity of nanosuspensions, Arch. Mater. Sci. 100 (2008) 99–104.

[16] L.S. Sundar et al., Thermal conductivity and viscosity of Fe_3O_4 nanofluid, Int. Commun. Heat Mass Transf. 44 (2013) 7–14. https://doi.org/10.1016/j.icheatmasstransfer.2013.02.014

[17] M.J. Pastoriza-Gallego et al., Al_2O_3–EG nanofluids, Nanoscale Res. Lett. 6 (2011) 221. https://doi.org/10.1186/1556-276X-6-221

[18] M. Pastoriza-Gallego et al., ZnO–EG nanofluids, J. Chem. Thermodyn. 73 (2014) 23–30. https://doi.org/10.1016/j.jct.2013.07.002

[19] M. Akbari et al., Rheological behavior of EG-based nanofluids, J. Mol. Liq. 233 (2017) 352–357. https://doi.org/10.1016/j.molliq.2017.03.020

[20] D. Kwek et al., Thermal property measurements of nanofluids, J. Chem. Eng. Data 55 (2010) 5690–5695. https://doi.org/10.1021/je1006407

[21] H.E. Patel et al., Thermal conductivity enhancement, J. Nanopart. Res. 12 (2010) 1015–1031. https://doi.org/10.1007/s11051-009-9658-2

[22] W. Duangthongsuk, S. Wongwises, TiO_2–water nanofluids, Exp. Therm. Fluid Sci. 33 (2009) 706–714. https://doi.org/10.1016/j.expthermflusci.2009.01.005

[23] I. Akande et al., Dispersion factor model for nanofluids, J. Mol. Liq. 380 (2023) 121644. https://doi.org/10.1016/j.molliq.2023.121644

[24] M. Klazly, G. Bognár, Empirical equation for nanofluid viscosity, Int. Commun. Heat Mass Transf. 135 (2022) 106054. https://doi.org/10.1016/j.icheatmasstransfer.2022.106054

[25] S.M. Hosseini et al., Dimensionless group model, J. Therm. Anal. Calorim. 100 (2010) 873–877. https://doi.org/10.1007/s10973-010-0721-0

[26] G.K. Batchelor, Effect of Brownian motion, J. Fluid Mech. 83 (1977) 97–117. https://doi.org/10.1017/S0022112077001062

[27] R.L. Hamilton, O. Crosser, Thermal conductivity of heterogeneous systems, Ind. Eng. Chem. Fundam. 1 (1962) 187–191. https://doi.org/10.1021/i160003a005

[28] R. Prasher et al., Brownian-motion-based model, J. Heat Transf. 128 (2006) 588–595. https://doi.org/10.1115/1.2188509

[29] A. Moghadassi et al., Dimensionless thermal conductivity model, J. Therm. Anal. Calorim. 96 (2009) 81–84. https://doi.org/10.1007/s10973-008-9843-z

[30] M. Hosseini et al., Local composition theory for nanofluids, J. Heat Transf. 133 (2011) 052401. https://doi.org/10.1115/1.4003042